Laser-based continuous-wave excitonic Lyman spectroscopy in Cu_2O

Kosuke Yoshioka, Takuro Ideguchi, and Makoto Kuwata-Gonokami*
Department of Applied Physics, The University of Tokyo, and Solution Oriented Research for Science and Technology (SORST), JST, 7-3-1 Hongo, Bunkyo-ku, Tokyo 113-8656, Japan

(Received 28 March 2007; revised manuscript received 26 May 2007; published 30 July 2007)

We developed continuous-wave, laser-based excitonic Lyman spectroscopy for sensitive and wide dynamic range detection of 1*s* paraexcitons in Cu_2O. A single-line tunable carbon dioxide laser was used as a probe light source. The minimum detectable induced transmission change was of the order of 10^{-5}, allowing us to accurately measure the induced absorption spectra of paraexcitons in thermal equilibrium with the lattice in a low-density limit. Using this spectroscopy technique, we measured important basic parameters, such as the effective mass and lifetime of paraexcitons, that are crucial for discussing the possibility of reaching a Bose-Einstein condensation state with this elementary excitation in a solid.

DOI: 10.1103/PhysRevB.76.033204 PACS number(s): 71.35.Cc, 71.35.Lk, 42.62.Fi

1*s* paraexcitons in Cu_2O are promising candidates for excitonic Bose-Einstein condensation in thermal equilibrium with the lattice. Due to the parity-forbidden band structure and pure spin-triplet nature, paraexcitons have a long lifetime that is sufficient to reach thermal equilibrium. However, these characteristics, in turn, mean very small radiative efficiency so that a poor signal-to-noise ratio is obtained with conventional luminescence measurements. This fact has hindered optical measurements of the effective mass of paraexcitons and their lifetime, and even their existence itself has been elusive. For 1*s* orthoexcitons the effective mass can be deduced by analyzing thermalization kinetics observed from their rather strong luminescence,[1–3] but for paraexcitons this method is not possible. For the lifetime, reported values based on luminescence measurements vary widely, from a nanosecond to a microsecond time range.[4–6] It is commonly believed that the lifetime is limited by impurity or vacancy concentration. In the case of low detection efficiency, however, one may measure a rather high density of paraexcitons with a decay time that is limited by collision-induced nonradiative decay processes. Therefore, it is necessary to determine experimentally basic parameters such as the effective mass and the lifetime of paraexcitons by developing a wide dynamic range method to detect low-density paraexcitons in thermal equilibrium.

Recently, excitonic Lyman spectroscopy has been attracting attention as a sensitive detection method using hydrogen-like internal transitions.[7–13] Earlier works on excitonic internal transitions can be found for, e.g., Si,[14] Ge,[15,16] and GaAs quantum wells.[17] We have studied the exciton dynamics in the time range of picoseconds to nanoseconds using femtosecond midinfrared pump-probe spectroscopy.[7,8,11,13] This spectroscopy can detect orthoexciton and paraexciton densities separately and quantitatively, but the dynamic range is limited.

In this Brief Report, we report on sensitive excitonic Lyman spectroscopy based on continuous-wave laser light sources. With this technique, we could detect a transmission change of the order of 10^{-5}, which is about 2 orders of magnitude better than lamp-based Fourier transform infrared (FTIR) spectroscopy.[9,12] This enabled us to observe in a low-density limit 1*s* paraexcitons in thermal equilibrium with the lattice and to measure their effective mass. In addition, we directly measured the lifetime of paraexcitons by monitoring the excitonic Lyman absorption and compared it with a luminescence measurement to confirm the reliability of the method.

Figure 1(a) is a simplified schematic of the experimental setup. The sample is a high-quality natural single crystal and its thickness is 220 μm. The excitation light is provided by a rhodamine 6G ring dye laser. The excitation wavelength is 601 nm (2.064 eV, 30 meV above the 1*s* orthoexciton resonance), which excites 1*s* orthoexcitons via an indirect phonon-assisted absorption process. The measured absorption coefficient at 5 K is 22 cm^{-1}. 1*s* paraexcitons are generated by a phonon-assisted down-conversion process[5,6,18,19] from the orthoexcitons. The excitation beam is intensity modulated by a glass acousto-optic modulator (AOM). The average power after passing through the AOM is stabilized so that the paraexciton density is constant during the measurements. The probe light source is a grating tunable single-line selective carbon dioxide (CO_2) laser. As shown in Fig. 1(b), the 9P branch lines spectrally coincide with the 1*s*-2*p* resonance of paraexcitons, allowing us to obtain induced absorption spectra with accurate wavelength values. Here, we focus only on paraexcitons as we can expect very weak signal for orthoexcitons due to small Boltzmann factors for our temperatures set and our low excitation densities. The probe beam is intensity modulated by a germanium AOM. To ensure that the absorption regime is linear, a probe beam that is much weaker than the excitation beam is used. The excitation and probe beams are spatially overlapped and focused by an off-axis parabolic mirror onto the Cu_2O sample in a dynamic flow cryostat. In front of the sample, we put an aperture mask with a 200 μm diameter to ensure spatial overlap between the excitation and probe beams. After transmission through the sample, the midinfrared probe beam is detected by a photovoltaic mercury cadmium telluride (MCT) detector. The signal from the MCT detector is sent into two lock-in amplifiers.

The wave form of the amplitude modulation applied is a 50% duty ratio square wave and the repetition frequencies are 5 kHz (f) and 10 kHz ($2f$) for the excitation and probe beams, respectively. The paraexciton gas reaches a steady-state regime in a much shorter time scale. The intensity of

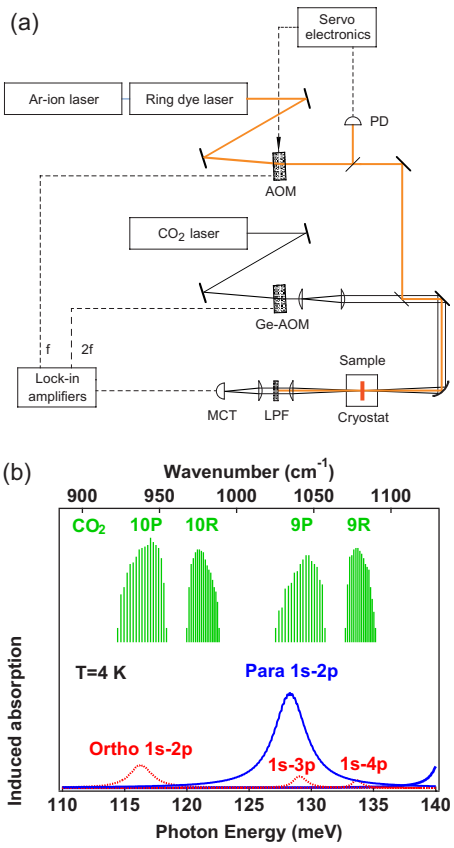

FIG. 1. (Color online) (a) Experimental setup. Both excitation and probe beams are modulated by acousto-optic modulators (AOMs). The average power of the excitation beam is stabilized by monitoring using a photodetector (PD). After transmitting a Cu_2O sample in a dynamic flow cryostat, the excitation beam is cut by a long pass filter (LPF) and the probe beam is detected by a mercury cadmium telluride (MCT) detector. The voltage signal from the MCT detector is sent into two lock-in amplifiers and two frequency components (f and $2f$) are extracted simultaneously. (b) Spectral position of CO_2 laser lines (upper part) and calculated induced absorption spectra of paraexcitons and orthoexcitons at 4 K (lower part).

the probe beam is monitored as the $2f$ component $[V(2f)]$ of the lock-in amplifier and the $1s$-$2p$ induced absorption of paraexcitons appears as the f component $[V(f)]$. The differential transmission is calculated using the equation $-\Delta T/T = -2V(f)/[V(f)+\sqrt{2}V(2f)]$. We repeat this procedure for each probe wavelength to obtain the induced absorption spectrum. The minimum transmission change obtained in this experiment is about 3×10^{-5} and is limited by our observation bandwidth and the dynamic reserve of the lock-in amplifier. The paraexciton density can be estimated from the induced absorption area assuming a $1s$-$2p$ dipole moment of 4.2 e Å.[11] The estimated paraexciton density at 4 K with this minimum transmission change is 5×10^{11} cm^{-3}.

The excitonic Lyman spectroscopy allows us to measure the thermal distribution of $1s$ excitons because of different effective masses of $1s$ and $2p$ excitons.[7] Thus, under fixed exciton temperatures we can evaluate the effective mass of $1s$ excitons. Here, we describe the procedure. The circles in Fig. 2 show a typical differential transmission spectrum

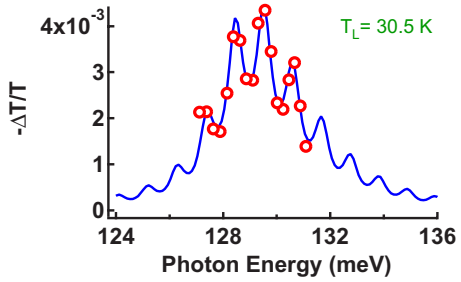

FIG. 2. (Color online) Typical differential transmission spectrum taken at 30.5 K. (Open circles) Experimental data. The absorbed excitation intensity is 7.4 W/cm^2. The upper bound of the power density of our probe beam is about 50 mW/cm^2. The oscillatory structure is due to a Fabry-Pérot interference effect in the sample. (Solid curve) A theoretical fitting assuming equal exciton temperature with the lattice (see text).

taken at 30.5 K. The absorbed excitation intensity is 7.4 W/cm^2. The spectral oscillatory structure is due to the Fabry-Pérot interference effect in the sample. The solid curve is a theoretical fitting curve and its details are as follows. The theoretical spectral function assuming a Maxwell-Boltzmann distribution of the $1s$ excitons is

$$\Delta\alpha(E) \propto \int \sqrt{E-E_0-\epsilon}\exp\left(-\frac{E-E_0-\epsilon}{(m_{1s}/m_{2p}-1)k_BT}\right) \times \frac{\Gamma_{2p}/2}{\epsilon^2+(\Gamma_{2p}/2)^2}d\epsilon, \quad (1)$$

where E, E_0, m_{1s}, and m_{2p} are the energy of the probe light, offset energy of the $1s$-$2p$ transition, effective mass of $1s$ excitons, and effective mass of $2p$ excitons, respectively. The linewidth of $2p$ exciton level is taken into account by convoluting the Boltzmann distribution with a Lorentzian function whose full width at half maximum is Γ_{2p}. $m_{2p}=1.68m_e$ (Ref. 20) is a sum of the effective masses of an electron and a hole (m_e is the free electron mass). The line shape function is discussed in detail in Refs. 12 and 21. We assumed the temperature of the exciton gas T to be the same as that of the lattice (thermal equilibrium). The fitting parameters are thus m_{1s}, E_0, Γ_{2p}, the thickness of the sample, and the imaginary part of the background index of refraction. The real part of the index is also included using a Sellmeier equation. As can be seen in Fig. 2, a reasonably accurate fit is obtained assuming $T=30.5$ K, and the resultant effective mass of $1s$ paraexcitons is $m_{1s\text{-}para}=(2.38\pm0.28)m_e$. Figure 3(a) shows induced absorption spectra taken at different temperatures from 5.1 to 30.5 K. Applying the same temperature between the exciton gas and the lattice gives a reasonable fit for each spectrum. This fact shows that our cw excitonic Lyman spectroscopy detects $1s$ paraexcitons in thermal equilibrium with the lattice. The effective mass of $1s$ paraexcitons extracted from each spectrum is shown in Fig. 3(b). The effective mass of $1s$ paraexciton deduced from our spectroscopy is $m_{1s\text{-}para}=(2.40\pm0.34)m_e$, assuming that it is temperature independent. All of the errors reported here are evaluated with a 95% confidence level. By comparison, the effective mass of $1s$ orthoexcitons is $2.7m_e$.[2] From recent high resolution

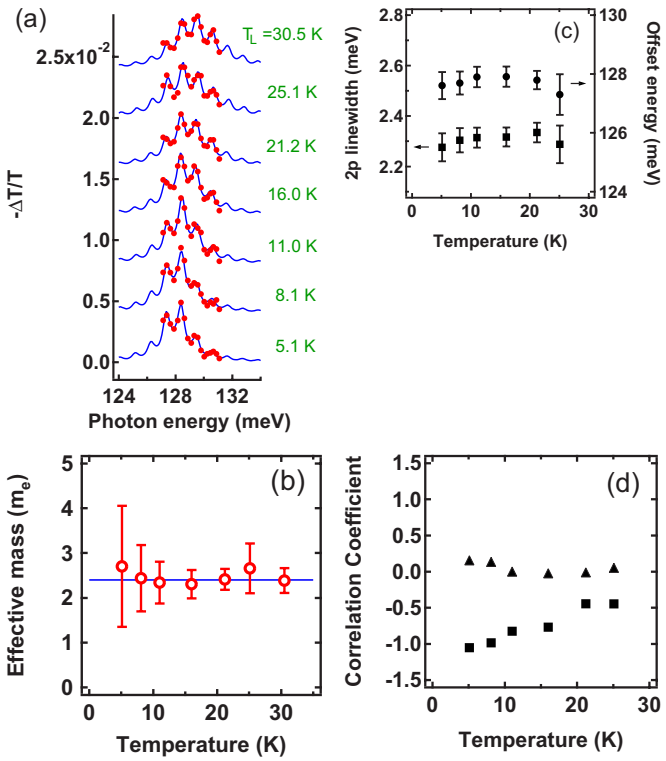

FIG. 3. (Color online) (a) Differential transmission spectra of the $1s$-$2p$ transition of paraexcitons as a function of lattice temperature T_L. Closed circles are experimental data. The absorbed excitation intensity is 7.4 W/cm^2 for every temperature. Solid curves show theoretical fitting as in Fig. 2. (b) Effective mass of the $1s$ paraexciton extracted from each spectrum shown in (a). Assuming a temperature-independent mass, the effective mass is estimated to be $(2.40\pm0.34)m_e$ (shown as a solid line). (c) Linewidth of $2p$ exciton level Γ_{2p} (closed squares) and offset energy of the $1s$-$2p$ transition E_0 (closed circles) that are obtained in our theoretical fittings. (d) Correlation coefficients between the effective mass of $1s$ excitons m_{1s} and Γ_{2p} (closed squares), and between m_{1s} and the thickness of the sample (closed triangles).

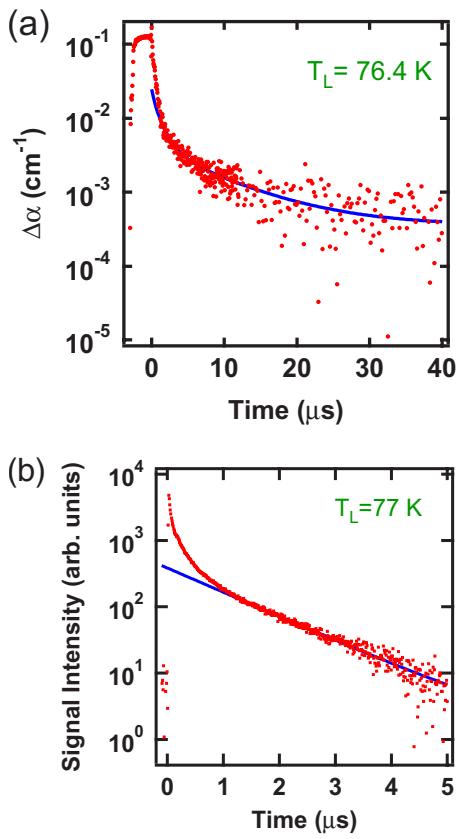

FIG. 4. (Color online) Time-resolved signal of the induced absorption at 9639 nm (dots). The lattice temperature is 76.4 K. The solid curve shows theoretical fitting with a double exponential function taking into account the two-dimensional spatial diffusion (see text). The decay constants are 1.92 ± 0.81 and 8.94 ± 3.93 μs. (b) Time-resolved signal of the Γ_3^- phonon-assisted luminescence of $1s$ orthoexcitons at 77 K under femtosecond two-photon interband excitation. A theoretical fitting with a single exponential function gives a decay time of 1.18 ± 0.04 μs.

absorption measurements on the temperature dependence of paraexciton linewidth under a high magnetic field, a $2.61m_e$ effective mass was estimated.[22] Lamp-based FTIR experiments suggest a temperature-dependent effective mass of $(2.2\pm0.1)m_e$ in our temperature range and a smaller mass at higher temperature.[12] Our estimation is in agreement with these values.

Here, we evaluate other parameters that we obtained in the fittings and show how they contribute to the errors of m_{1s}. Shown in Fig. 3(c) are Γ_{2p} and E_0, which have a large effect on the evaluation of m_{1s}. In Fig. 3(d), we show correlation coefficients evaluated between m_{1s} and other parameters. E_0 is covariant with m_{1s} as can be seen in Eq. (1). Other than this, Γ_{2p} has negative covariance with m_{1s} especially at low temperatures. This is due to the thermal broadening of the $1s$ level becoming comparable to the $2p$ linewidths. This fact contributes to the relatively large error bars at low temperatures in Fig. 3(b). On the contrary, the interference fringe (the thickness of the sample) has little effect on the effective mass of paraexcitons.

Next, we measured the lifetime of paraexcitons using the $1s$-$2p$ induced absorption. For this purpose, we applied small duty ratios for both excitation and probe light so that their pulse duration are 3 μs and 70 ns, respectively. The latter limits the time resolution for this measurement. The repetition rates are 5 and 10 kHz for the excitation and probe pulses, respectively. The minimum detectable transmission signal change is 1×10^{-5}. The wavelength of the probe light is fixed at 9639 nm (128.6 meV).

Figure 4(a) shows the time-resolved induced absorption signal taken at 76.4 K. There are three characteristic time regions. In an early time range up to about 1 μs, a rapid decay is observed and is due to a two-body collision-induced loss process.[5,23–25] After this rapid initial decay, the signal decreases double exponentially with a faster component originating from the lifetime of paraexcitons and a slower component attributed to impurity-bound excitons.[12,26] This difference can clearly be observed in the induced absorption spectra taken at each characteristic time, which is not discussed here. When discussing the long lifetime of paraexcitons, one has to carefully treat spatial diffusion.[27] In our experiment, the aperture mask of 200 μm diameter results in an apparently rapid decay of paraexcitons. The diffusion co-

efficient at this lattice temperature is $D=18\ \mathrm{cm}^2/\mathrm{s}$.[28] The decay curve considering the spatial escape from our observation region can be written as $\Delta\alpha(t)=d(t)A_f\exp(-t/\tau_f)+A_b\exp(-t/\tau_b)$, where $\Delta\alpha(t)$ is the induced absorption coefficient, $A_{f(b)}$ is the signal amplitude due to free (bound) excitons, and $\tau_{f(b)}$ is the lifetime of free (bound) excitons. $d(t)$ represents a numerically calculated decay taking into account the two-dimensional spatial diffusion. A least-squares fit (between 1.2 and 40 μs) using the above equation gives $\tau_f=1.92\pm0.81$ μs and $\tau_b=8.94\pm3.93$ μs. For comparison, a time-resolved signal of the Γ_3^- phonon-assisted luminescence of 1*s* orthoexcitons at 77 K for the same sample is shown in Fig. 4(b). The excitation light source is the 200 kHz regenerative amplification of a femtosecond Ti:S laser, and 1*s* excitons are generated after an interband two-photon absorption process.[9] At this high temperature, the populations of orthoexcitons and paraexcitons are in thermal equilibrium so that the effective paraexciton lifetime can be observed by Γ_3^- luminescence. The paraexciton lifetime at this temperature is mostly limited by the intrinsic lifetime of orthoexcitons for high purity samples. A least-squares fit (between 1.2 and 5 μs) to a single exponential gives a 1.18 ± 0.04 μs lifetime, confirming our direct measurement by excitonic Lyman spectroscopy. This method must be distinctly important at low temperatures below 20 K where the indirect observation of paraexcitons via orthoexciton luminescence does not work.

In conclusion, we developed cw laser-based excitonic Lyman spectroscopy for sensitive detection of low density and thermal equilibrium 1*s* paraexcitons in Cu_2O. We improved our detection dynamic range from 3 to 5 orders of magnitude in the midinfrared and a dilute paraexciton gas with a density of the order of $10^{11}\ \mathrm{cm}^{-3}$ was observed. Using this technique, we measured the thermal distribution of paraexcitons in equilibrium, and we determined the effective mass of paraexcitons to be $(2.40\pm0.34)m_e$ from a line shape analysis. We also measured the lifetime of spin-forbidden paraexcitons directly using the excitonic Lyman spectroscopy in a tens of microseconds time scale. The wide dynamic range of our method will allow one to investigate the density-dependent exciton loss mechanism with unambiguous knowledge of the paraexciton density. In addition, it is possible that quantum cascade lasers, which have been rapidly developing recently, will match this spectral region. This continuously tunable probe light source will allow one to conduct much more precise measurements of important parameters such as the effective mass.

We thank A. Mysyrowicz for fruitful discussions and supplying the high-quality sample. We also thank J. B. Héroux for critical reading of the Brief Report. This work is partly supported by the Grant-in-Aid for Scientific Research (S) from Japan Society for the Promotion of Science (JSPS).

*gonokami@ap.t.u-tokyo.ac.jp

[1] P. Y. Yu and Y. R. Shen, Phys. Rev. Lett. **32**, 939 (1974).
[2] N. Caswell, J. S. Weiner, and P. Y. Yu, Solid State Commun. **40**, 843 (1981).
[3] D. W. Snoke, D. Braun, and M. Cardona, Phys. Rev. B **44**, 2991 (1991).
[4] A. Mysyrowicz, D. Hulin, and A. Antonetti, Phys. Rev. Lett. **43**, 1123 (1979).
[5] S. Denev and D. W. Snoke, Phys. Rev. B **65**, 085211 (2002).
[6] J. I. Jang, K. E. O'Hara, and J. P. Wolfe, Phys. Rev. B **70**, 195205 (2004).
[7] M. Kuwata-Gonokami, M. Kubouchi, R. Shimano, and A. Mysyrowicz, J. Phys. Soc. Jpn. **73**, 1065 (2004).
[8] M. Kubouchi, K. Yoshioka, R. Shimano, A. Mysyrowicz, and M. Kuwata-Gonokami, Phys. Rev. Lett. **94**, 016403 (2005).
[9] K. Karpinska, P. H. M. van Loosdrecht, I. P. Handayani, and A. Revcolevschi, J. Lumin. **112**, 17 (2005).
[10] M. Jörger, T. Fleck, and C. Klingshirn, J. Lumin. **112**, 21 (2005).
[11] T. Tayagaki, A. Mysyrowicz, and M. Kuwata-Gonokami, J. Phys. Soc. Jpn. **74**, 1423 (2005).
[12] M. Jörger, T. Fleck, C. Klingshirn, and R. von Baltz, Phys. Rev. B **71**, 235210 (2005).
[13] T. Tayagaki, A. Mysyrowicz, and M. Kuwata-Gonokami, Phys. Rev. B **74**, 245127 (2006).
[14] D. Labrie, M. L. W. Thewalt, I. J. Booth, and G. Kirczenow, Phys. Rev. Lett. **61**, 1882 (1988).
[15] E. M. Gershenzon, G. N. Gol'tsman, and N. G. Ptitsina, Zh. Eksp. Teor. Fiz. **70**, 224 (1976) [Sov. Phys. JETP **43**, 116 (1976)].
[16] T. Timusk, Phys. Rev. B **13**, 3511 (1976).
[17] R. H. M. Groeneveld and D. Grischkowsky, J. Opt. Soc. Am. B **11**, 2502 (1994).
[18] N. Caswell and P. Y. Yu, Phys. Rev. B **25**, 5519 (1982).
[19] D. W. Snoke, D. P. Trauernicht, and J. P. Wolfe, Phys. Rev. B **41**, 5266 (1990).
[20] J. W. Hodby, T. E. Jenkins, C. Schwab, H. Tamura, and D. Trivich, J. Phys. C **9**, 1429 (1976).
[21] K. Johnsen and G. M. Kavoulakis, Phys. Rev. Lett. **86**, 858 (2001).
[22] D. Fröhlich (private communication).
[23] K. E. O'Hara and J. P. Wolfe, Phys. Rev. B **62**, 12909 (2000).
[24] J. I. Jang and J. P. Wolfe, Phys. Rev. B **74**, 045211 (2006).
[25] Y. Liu and D. Snoke, Solid State Commun. **140**, 208 (2006).
[26] J. I. Jang, Y. Sun, B. Watkins, and J. B. Ketterson, Phys. Rev. B **74**, 235204 (2006).
[27] T. Fleck, M. Jörger, and C. Klingshirn, Phys. Status Solidi C **3**, 2473 (2006).
[28] D. P. Trauernicht and J. P. Wolfe, Phys. Rev. B **33**, 8506 (1986).